



## Structure, composition and corrosion resistance studies of Co–Cr alloy electrodeposited from deep eutectic solvent (DES)

Gengan Saravanan, Subramanian Mohan\*

EMFT Division, CSIR – Central Electrochemical Research Institute, Karaikudi 630006, India

### ARTICLE INFO

#### Article history:

Received 27 June 2011

Received in revised form 23 January 2012

Accepted 24 January 2012

Available online 2 February 2012

#### Keywords:

Coating materials

Crystal growth

Crystal structure

Corrosion

Electrochemical impedance spectroscopy

X-ray diffraction

### ABSTRACT

Electrodeposition of Co–Cr alloys on brass and mild steel substrates has been investigated using direct current (DCD) and pulsed electrodeposition (PED) techniques. The alloy contains approximately 65–81% Co, and 19–35% Cr. The aim of this work is to develop a stable deep eutectic solvent (DES) containing Co(II), and Cr(III) ion without any Cr complexing agent. The influences of direct current and pulsed current on the Co–Cr compositions have been investigated. The crystallographic structures, morphology and chemical composition of Co–Cr deposited films are analyzed by means of XRD, SEM, EDS and XPS. The anticorrosive properties of  $\text{Co}_{80.04}\text{Cr}_{19.95}$  (DCD) and  $\text{Co}_{65.44}\text{Cr}_{34.55}$  (PED) alloy on mild steel substrate have been studied and compared using potentiodynamic polarization and electrochemical impedance spectroscopy.

© 2012 Elsevier B.V. All rights reserved.

### 1. Introduction

Cobalt and chromium is one of the most important constituents of functional materials for excellent corrosion and wear-resistant alloys. Co–Cr alloys are widely used for medical prosthetic implant devices, such as knee implants, metal-to-metal hip joints and dental prosthetics [1]. Preparation of Co–Cr alloy from aqueous based electrolyte is suffered by  $\text{H}_2$  embrittlement, olation and narrow electrochemical potential windows of water. Room temperature ionic liquids (RTILs) are promising electrolytes for the electrodeposition of various metals and alloys because of their wide electrochemical potential windows, nonvolatility and high thermal stability [2–6]. Recently alternative class of materials is based on combination of choline chloride (2-hydroxy-N,N,N-trimethylethanminium chloride) with hydrogen bond forming compounds, such as urea or ethylene glycol (EG) was investigated by many researchers [7–10]. 1:1:0.5:2 M ratio of choline chloride,  $\text{CrCl}_3 \cdot 6\text{H}_2\text{O}$ ,  $\text{CoCl}_2 \cdot 6\text{H}_2\text{O}$  and ethylene glycol mixtures form a deep eutectic solvent (DES) which exhibit some properties similar to RTILs.

Non-precious metals and alloys (Co–Cr, Ni–Cr) are recent trend replacing precious or noble alloy in dentistry. Almost 90% of all removable partial dentures are now cast from non-precious alloys

containing Co, Cr, Ni [11]. These alloys posses better mechanical properties, therefore can be easily cast into desired thinner shapes in oral cavity, the salinity of saliva approaches that of seawater and tends to be highly corrosive to most non-noble metals [11]. The pH of saliva may vary between 3 and 10 while the temperature in the oral cavity may be between 5 and 70 °C, all these variations mostly depends on the food intake [12]. The corrosion resistance in addition to other consideration such as affordability, biocompatibility and mechanical properties of alloys [13–15] plays an important role.

In designing non-precious alloys, Cr is added in the range of 10–30% to obtain an optimum value of corrosion resistance and mechanical strength. A review of literature reveals various studies on alloys. Ameer et al. have studied potentiodynamic polarization and electrochemical impedance behavior of Co–Cr, Ni–Cr, and concluded that Co–Cr–Mo alloys are more resistance to corrosion as compared to Ni–Cr–Mo alloys [16]. The presence of Cr improves the corrosion resistance of alloys in a corrosive environment due to the formation of a Cr–rich, passive oxide film which is highly resistant to acid attack. Similarly, presence of iron in the Ni–Cr based alloy increases the resistance to localized corrosion in the chloride-containing environment [17]. Therefore, for Ni–Cr based alloy, the addition of 12% Cr and 2–5% Mo to the alloy bulk is well recommended from the corrosion resistance point of view.

The purpose of this work was to show important results on structural morphology and composition of Co–Cr alloy deposited by DCD and PED in choline chloride based deep eutectic solvent.

\* Corresponding author. Tel.: +91 4565 227551; fax: +91 4565 227713.  
E-mail addresses: [mohan40159@cecri.res.in](mailto:mohan40159@cecri.res.in), [sanjnamohan@yahoo.com](mailto:sanjnamohan@yahoo.com) (S. Mohan).

Significant of this work is in terms of free from aqueous electrolyte, no complexing agent, absence of  $H_2$  evolution, without additives like saccharine and sodium lauryl sulphate. Potentiodynamic polarization and electrochemical impedance spectroscopy technique were used to study the anticorrosive properties of  $Co_{80.04}Cr_{19.95}$  and  $Co_{65.44}Cr_{34.55}$  alloy.

## 2. Experimental details

### 2.1. Preparation of deep eutectic solvent and electrochemical deposition

The deep eutectic solvent (DES) was prepared by mixing 1 M choline chloride, 1 M  $CrCl_3 \cdot 6H_2O$ , 0.5 M  $CoCl_2 \cdot 6H_2O$ , 0.5 M KCl, 2 M ethylene glycol at 65 °C until a homogeneous liquid was formed. The alloys were deposited on polished and electrocleaned brass and mild steel substrate under continuous stirring. Graphite is used as the anode, brass and mild-steel plates were used as the cathode. The samples obtained by DCD and PED alloy were represented as  $Co_{80.04}Cr_{19.95}$  – (DCD)/MS and  $Co_{65.44}Cr_{34.55}$  – (PED)/MS. Pulse electrodeposition was done using Dynatronix (USA) DPR20-5-10 Model. The pulse parameters and formula used were given in our previous studies [18].

### 2.2. Corrosion resistance studies and structural morphology

Potentiodynamic polarization and electrochemical impedance spectroscopy (EIS) studies of alloy electrodeposits obtained by DCD and PED on mild steel substrate were done in 3.5% NaCl solution. Potentiodynamic polarization curves were measured for electrodeposited alloy between  $-0.25$  and  $0.25$  V at scan rate of  $5 \text{ mV s}^{-1}$ . The corrosion resistance parameters were obtained with inbuilt software (Power Suite). EIS were conducted at open circuit potential over a frequency range from  $10^5$  to  $10^{-2}$  Hz. The amplitude of potential modulation was 5 mV. All the recorded impedance spectra were shown as Nyquist diagram.

Microstructural characterizations were carried out using scanning electron microscopy equipped with energy dispersive X-ray spectroscopy (Hitachi, 3000H). X-ray diffraction pattern of alloy phases was measured using a PANalytical model

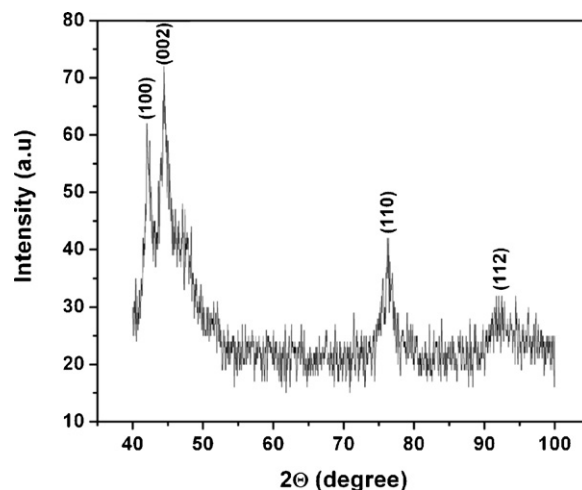


**Fig. 1.** XRD pattern of  $Co_{65.44}Cr_{34.55}$  – PED alloy at an average current density of  $15 \text{ A dm}^{-2}$  in deep eutectic solvent.

X'pert PRO X-ray diffractometer,  $2\theta$  from 20 to 100 using  $Cu \text{ K}\alpha$ ,  $\lambda=0.1540 \text{ nm}$ . X-ray photoelectron spectroscopy (XPS) of as electrodeposited Co–Cr alloy was investigated using VG electron spectroscopy. All spectra were recorded using an X-ray source (Al  $K\alpha$  radiation,  $E=1486 \text{ eV}$ ) with a scan range of 0–1200 eV binding energy. The collected high-resolution XPS spectra were analyzed using XPS peak fitting software program.

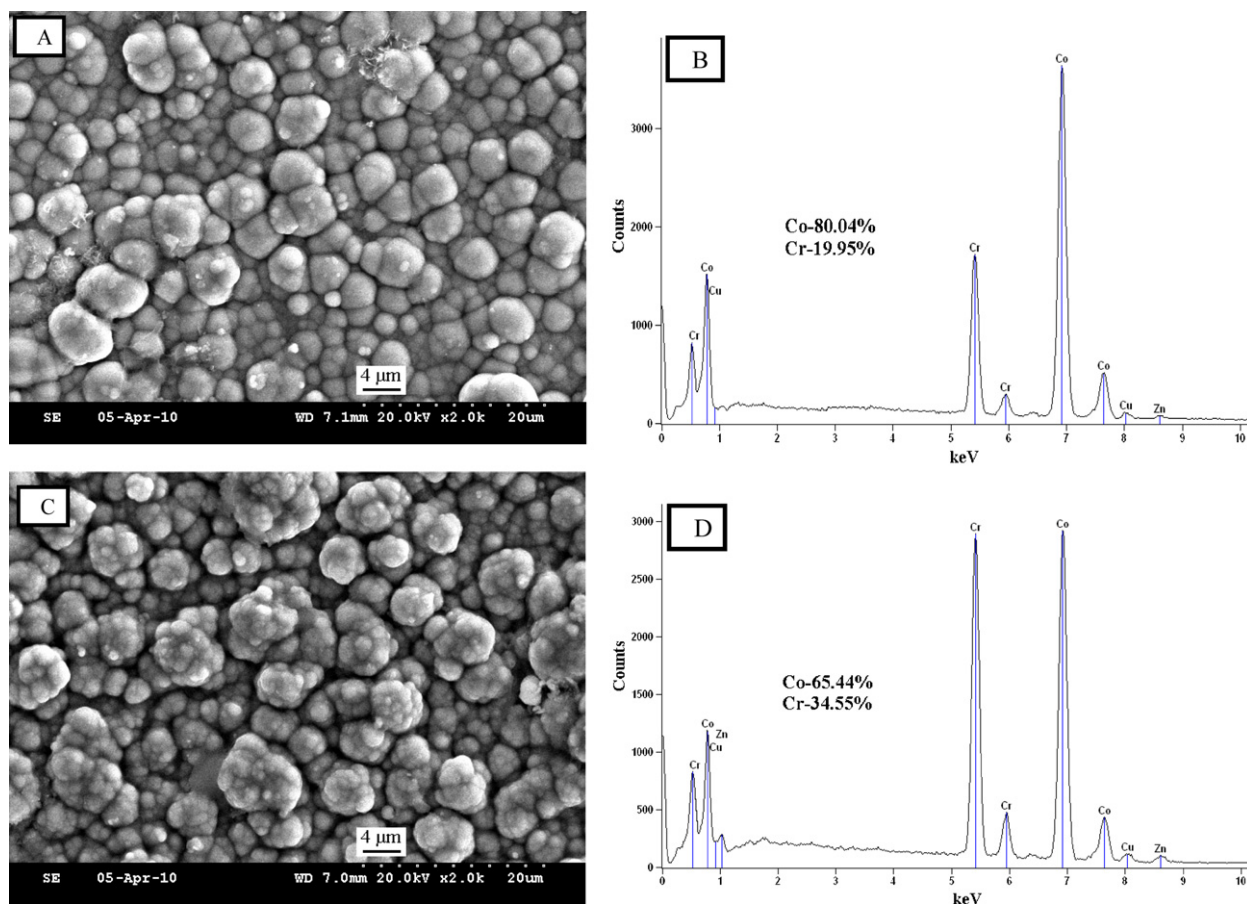


**Fig. 2.** SEM images and EDS patterns of  $Co_{80.04}Cr_{19.95}$  – DCD alloy at current density of  $15 \text{ A dm}^{-2}$  (A and B) and  $Co_{65.44}Cr_{34.55}$  – PED alloy at an average current density of  $15 \text{ A dm}^{-2}$ , 40 ms On-time, 60 ms Off-time and 25 Hz frequency (C and D).

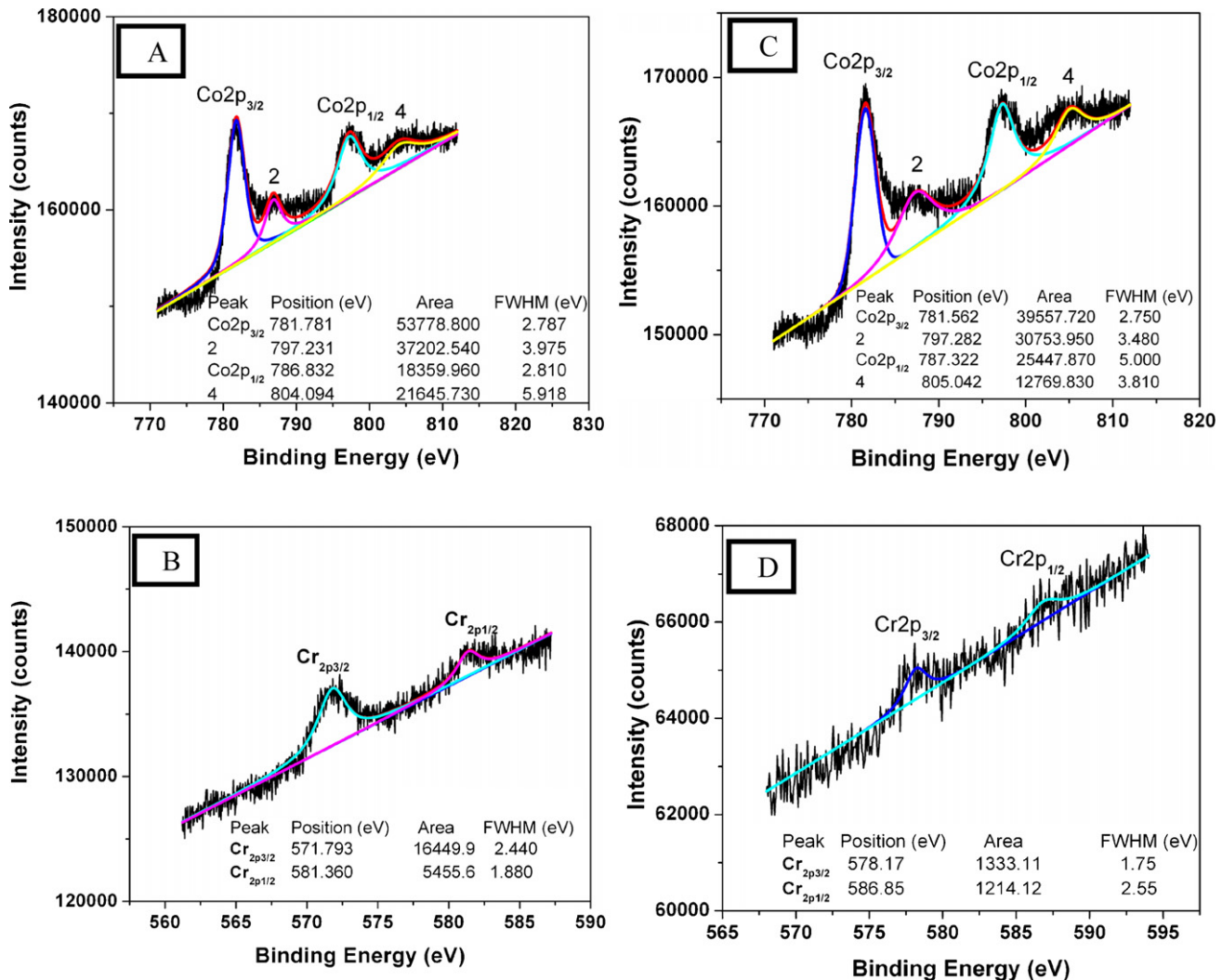


Fig. 3. X-ray photoelectron spectroscopy of Co–Cr alloy: (A) Co2p (PED), (B) Cr2p (PED), (C) Co2p (DCD) and (D) Cr2p (DCD).

### 3. Results and discussion

#### 3.1. X-ray diffraction analysis

The XRD patterns for Co–Cr alloy deposited in deep eutectic solvent are shown in Fig. 1. The pattern of the deposited alloy shows the presence of a hexagonal-close-packed (*hcp*) phase. The peaks were observed at diffraction angle of 42.17°, 44.44°, 76.29°, and 86.31° corresponding to (1 0 0), (0 0 2), (1 1 0), and (1 1 2) crystal planes and Co–Cr phases were polycrystalline. Which is quite consistent with reported literature [19]. The average crystallite size was estimated to be 28 nm by using Scherer formula [20].

#### 3.2. Microchemical and microstructural analyses

Direct current (DCD) and pulsed current (PED) have an important effect on structural morphology and composition of alloy deposits on brass/mild steel substrate. In the present study, the SEM images and EDS patterns show differences in the samples obtained by DCD and PED technique. Fig. 2A shows the morphology of alloy deposited at 15 A dm<sup>-2</sup> and the corresponding EDS pattern reveals the presence of Co–80.04% and Cr–19.95%. Deposits were nodular grain with sizes ranging from 2 to 4 μm without any agglomeration.

Fig. 2B shows the SEM and EDS results of alloy obtained at average current density ( $I_a$ ) of 15 A dm<sup>-2</sup>, these deposits were small

nodular with grain sizes ranging from 1 to 2.5 μm than those obtained by DCD technique. Deposits were denser and compact layer containing spherical particles, which formed as small clusters. The compositions of alloy atomic percentage were Co–65.44% and Cr–34.55% as shown by EDS analysis. PED alloy is having better structural morphology and observed the increase of Cr% in alloy composition than that of DCD alloy. From our previous studies maximum current efficiency is obtained at 40% duty cycle [21], so alloy depositions were also carried out at 40% duty cycle, 25 Hz frequency with an average current density ( $I_a$ ) of 15 A dm<sup>-2</sup>. At 40% duty cycle i.e. 40 ms On-time, 60 ms Off-time, when Off-time is higher, pulses are very short and they produce very thin pulsating diffusion layers. Diffusion of Cr ions from the bulk of the electrolyte to the electrode surface depends on gradient of Cr ions concentration. So at 40% duty cycle enhancement of migration of Cr ions increases the nucleation rate and uniformity of deposits [21]. Therefore, in PED of alloy obtained higher Cr percentage than that of DCD techniques.

#### 3.3. X-ray photoelectron spectroscopy studies

XPS analysis was performed to examine the elemental composition of Co<sub>80.04</sub>Cr<sub>19.95</sub> (DCD) and Co<sub>65.44</sub>Cr<sub>34.55</sub> (PED) alloy and to determine the valence states of elements, which indicated that the presence of Co2p<sub>1/2</sub>, Co2p<sub>3/2</sub>, Cr2p<sub>1/2</sub> and Cr2p<sub>3/2</sub> peaks (Fig. 3A–D). The chemical states were identified by comparison of the

photoelectron binding energies (BE) with those obtained from the literature [22,23]. The deconvoluted XPS spectra were treated by Linear-type background subtraction, mixed Gaussian/Lorentzian sum functions were used to construct symmetric peak shapes and peak decomposition using XPS peak fit software V 4.1. The peaks at binding energy about 781.7 and 786.8 eV correspond to  $\text{Co}2p_{3/2}$  and  $\text{Co}2p_{1/2}$  doublet and shake up resonance transition (satellite) of these two peaks at higher binding energies, indicates the presence of  $\text{Co}(0)$  [24]. It should be pointed out that the percentage of cobalt was found to be higher in the Co–Cr alloy deposited under PED than that of DCD (current density of  $15 \text{ A dm}^{-2}$ ). The spectrum of chromium exhibits the binding energy 571.7 and 581.3 eV corresponds to  $\text{Cr}2p_{3/2}$  and  $\text{Cr}2p_{1/2}$ , which are characteristics of metallic  $\text{Cr}(0)$  [25,26].

In particular, the intensity of the  $\text{Co}2p$  and  $\text{Cr}2p$  peaks in the spectra is proportional to the Co and Cr atomic concentration in the alloys [27,28]. The analysis of the  $\text{Co}2p$  and  $\text{Cr}2p$  peak intensities confirms the composition obtained by EDS within 3%. All the peaks in the spectra could be ascribed to either Co or Cr, which attests to the high purity and quality of the samples.

### 3.4. Potentiodynamic polarization studies

The results from the potentiodynamic polarization measurements of the  $\text{Co}_{80.04}\text{Cr}_{19.95}$  – (DCD) and  $\text{Co}_{65.44}\text{Cr}_{34.55}$  – (PED) alloy deposits on the mild steel (MS) substrates in the 3.5% NaCl are shown in Fig. 4A. The curves representing the bare substrates,  $\text{Co}_{80.04}\text{Cr}_{19.95}$  – (DCD) and  $\text{Co}_{65.44}\text{Cr}_{34.55}$  – (PED) on mild steel substrates were shown for comparison and the anticorrosive parameter values were given in Table 1. Among all the samples  $\text{Co}_{65.44}\text{Cr}_{34.55}$  – (PED) exhibits lesser negative value of ( $-0.502 \text{ V}$ ) corrosion potential ( $E_{\text{corr}}$ ) than  $\text{Co}_{80.04}\text{Cr}_{19.95}$  – (DCD) ( $-0.536 \text{ V}$ ) and MS substrate ( $-0.671 \text{ V}$ ). This indicates that after applying an alloy deposits obtained a better corrosion protection in both cases. Corrosion protection is normally proportional to the corrosion current density ( $I_{\text{corr}}$ ) measured via polarization. The very lower ( $I_{\text{corr}}$ ) values for the  $\text{Co}_{65.44}\text{Cr}_{34.55}$  – (PED)/MS ( $1.71 \times 10^{-6}$ ) and  $\text{Co}_{80.04}\text{Cr}_{19.95}$  – (DCD)/MS [29] ( $2.96 \times 10^{-6}$ ) than that of MS substrate ( $7.19 \times 10^{-4}$ ) indicate that the  $I_{\text{corr}}$  value of PED alloy is nearly 2 times lower than that of alloy obtained by DCD. Therefore, PED  $\text{Co}_{65.44}\text{Cr}_{34.55}$  alloy is more protective than DCD alloy and mild steel substrate. Corrosion rate in milli mils per year was estimated from the polarization curves, and given in Table 1. Very low corrosion rate is obtained for PED alloy deposits than that of DCD and bare substrate.

### 3.5. Electrochemical impedance spectroscopy measurements

The polarization resistance and double layer capacitance of Co–Cr deposits in a corrosive medium could provide information regarding the ongoing corrosion reaction process. EIS data provides additional information about the deposits/solution and substrate/solution interface. Fig. 4B shows the impedance response of Co–Cr alloy deposits and bare substrates in a Nyquist representation. At low frequencies the interception with the real axis was ascribed to the charge transfer resistance  $R_{\text{ct}}$  at the corrosion potential. The  $R_{\text{ct}}$  value of  $\text{Co}_{65.44}\text{Cr}_{34.55}$  – (PED)/mild steel

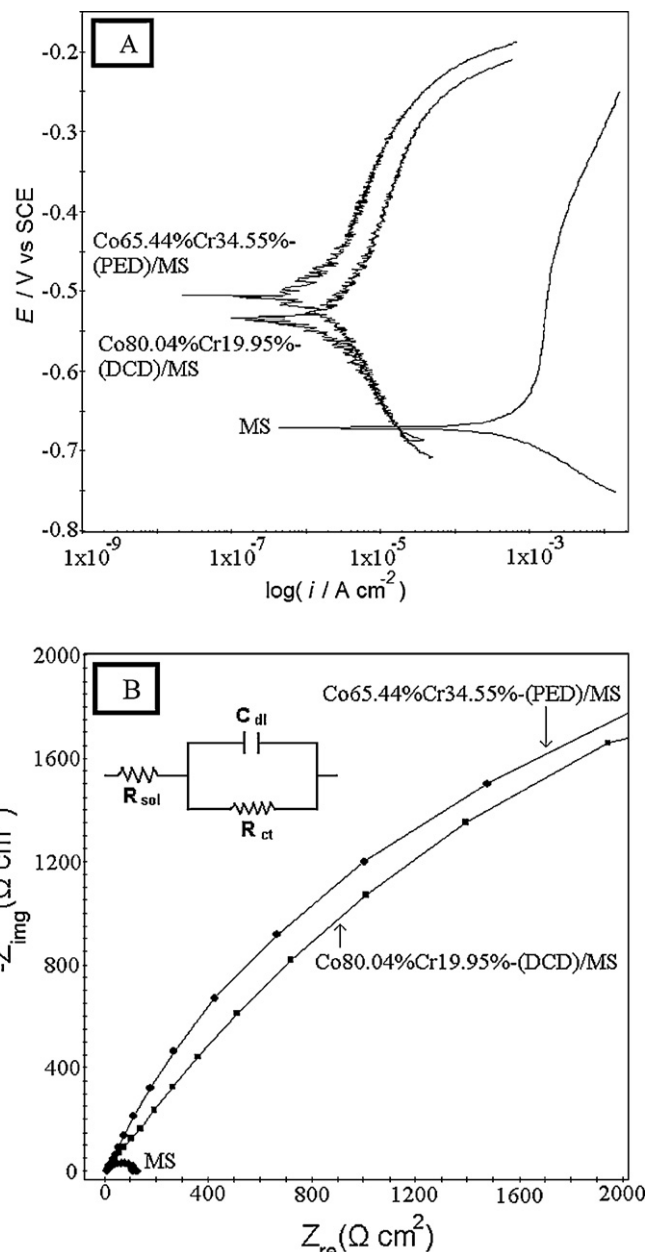


Fig. 4. (A) Typical potentiodynamic polarization curves of electrodeposited alloy and bare substrates in 3.5% NaCl solution. (B) Electrochemical impedance spectroscopy: Nyquist plot (insert equivalent circuit diagram for impedance spectra).

and  $\text{Co}_{80.04}\text{Cr}_{19.95}$  – (DCD)/mild steel were several orders of magnitude higher than that of bare mild steel substrate. The value of fitted parameters of the equivalent circuit, together with the corrosion potentials  $E_{\text{corr}}$  as a function of  $\text{Co}_{80.04}\text{Cr}_{19.95}$  – (DCD) and  $\text{Co}_{65.44}\text{Cr}_{34.55}$  – (PED) alloy electrodeposits on mild steel substrate were presented in Table 1. The double layer capacitance  $C_{\text{dl}}$  was another parameter that could provide information about the polarity and the amount of charge at the alloy deposits/solution

Table 1

Corrosion parameters obtained from polarization and electrochemical impedance measurements by Nyquist plot in 3.5% NaCl solution.

Sample	$E_{\text{corr}}$ vs (SCE)/mV	$b_a$ (V decade $^{-1}$ )	$b_c$ (V decade $^{-1}$ )	$I_{\text{corr}}$ (A cm $^{-2}$ )	Corrosion rate (mm y $^{-1}$ )	$R_{\text{ct}}$ ( $\Omega$ cm $^2$ )	$C_{\text{dl}}$ (F cm $^{-2}$ )
MS substrate	-0.671	0.373	-0.061	$7.19 \times 10^{-4}$	8.4294	131	$1.08 \times 10^{-3}$
$\text{Co}_{80.04}\text{Cr}_{19.95}$ – (DCD)/MS in DES	-0.536	0.220	-0.162	$2.96 \times 10^{-6}$	2.2207	8913	$1.30 \times 10^{-6}$
$\text{Co}_{65.44}\text{Cr}_{34.55}$ – (PED)/MS in DES	-0.502	0.198	-0.161	$1.71 \times 10^{-6}$	1.2690	12,810	$1.18 \times 10^{-6}$

interface. Higher  $E_{\text{corr}}$ ,  $R_{\text{ct}}$  and lower  $I_{\text{corr}}$ ,  $C_{\text{dl}}$  values of  $\text{Co}_{65.44}\text{Cr}_{34.55}$  – (PED) alloy electrodeposited on mild steel substrate showed better corrosion resistance properties than that of bare substrates.

#### 4. Conclusions

- We prepared a novel DES free from Cr-complexing agent, brighter and stress reducer for the electrodeposition of Co–Cr alloy.
- The effect of DCD and PED current on the structural morphology and composition of Co–Cr alloy was successfully studied by SEM, EDS and XPS techniques.
- By PED we were able to get 65.44% Co and 34.55% Cr whose structural morphology is fine grained.
- The potentiodynamic polarization and electrochemical impedance spectroscopy results showed  $\text{Co}_{65.44}\text{Cr}_{34.55}$ -alloy deposited by PED technique is having very higher  $R_{\text{ct}}$  and lower  $I_{\text{corr}}$  than that of  $\text{Co}_{80.04}\text{Cr}_{19.95}$  – (DCD) and bare mild steel substrate.

#### Acknowledgments

The authors wish to express sincere thanks to the Director, CECRI, Karaikudi-6 for his kind permission to publish these results. One of the authors, G. Saravanan thanks CSIR for the award of a Senior Research Fellowship. The authors also thank Mr. R. Ravishanker CECRI for SEM measurement.

#### References

- [1] <http://www.astm.org/> ASTM F75 Co–Cr alloy.
- [2] W. Simka, D. Puszczuk, G. Nawrat, *Electrochim. Acta* 54 (23) (2009) 5307.
- [3] M. Figueiredo, C. Gomes, R. Costa, *Electrochim. Acta* 54 (9) (2009) 2630.
- [4] A.N. Mao-Zhong, Y. Pei-Xia, S.U. Cai-Na, *Chin. J. Chem.* 26 (2008) 1219.
- [5] F. Endres, El Zein, S. Abedin, *Phys. Chem. Chem. Phys.* 8 (2006) 2101.
- [6] A.P. Abbott, K.J. McKennize, *Phys. Chem. Chem. Phys.* 8 (2006) 4265.
- [7] A.P. Abbott, G. Capper, D.L. Davies, *Chem. Commun.* 1 (2003) 70.
- [8] A.P. Abbott, D.L. Davies, G. Capper, *World Pat. WO 0226701* (2000).
- [9] A.P. Abbott, D. Boothby, G. Capper, *J. Am. Chem. Soc.* 126 (2004) 9142.
- [10] A. Bakkar, V. Neubert, *Electrochem. Commun.* 9 (2007) 2428.
- [11] J.C. Wataha, *J. Prosthet. Dent.* 87 (2002) 351.
- [12] J.F. McCabe, A.W.G. Walls, *Applied Dental Materials*, 8th ed., Munksgaard International Publishers, 1999.
- [13] J.C. Wataha, C.T. Hanks, Z. Sun, *Dent. Mater.* 11 (4) (1995) 239.
- [14] G. Schmalz, H. Langer, H. Schweikl, *J. Dent. Res.* 77 (10) (1998) 1772.
- [15] L. Reclaru, J.M. Meyer, *Biomaterials* 19 (1) (1998) 85.
- [16] M.A. Ameer, E. Khamis, M. Al-Motlaq, *Corros. Sci.* 46 (11) (2004) 2825.
- [17] G. Saravanan, S. Mohan, *J. Int. Electrochem. Sci.* 6 (2011) 1468.
- [18] G. Saravanan, S. Mohan, *Corros. Sci.* 51 (2009) 197.
- [19] N.B. Chaure, J.M.D. Coey, *J. Magn. Magn. Mater.* 303 (2006) 232.
- [20] H.P. Klug, L. Alexander, *Wiley-Interscience*, in: *X-ray Diffraction Procedures for Polycrystalline and Amorphous Material*, New York, 1980.
- [21] J.C.L. Puipe, F. Leaman, *Theory and Practice of Pulse Plating*, 1st ed., American Electroplaters and Surface Finishers Society, Orlando, FL, 1986, p. 247.
- [22] C.D. Wagner, W.M. Riggs, L.E. Davis, J.F. Moulder, G.E. Muilenberg, *Handbook of X-ray Photoelectron Spectroscopy*, Perkin-Elmer, Minneapolis, MN, 1978, p. 190.
- [23] C.D. Wagner, A.V. Naumkin, A. Kraut-Vass, J.W. Allison, C.J. Powell, J.R. Rumble Jr., *NIST Standard Reference Database 20*, Version 3.4 (Web Version).
- [24] B.-S. Jeong, Y.-M. Heo, D.P. Norton, *Appl. Phys. Lett.* 84 (14) (2004) 2608.
- [25] E. Desimoni, C. Malitesta, P.G. Zambonin, J.C. Riviere, *Surf. Interface Anal.* 13 (1988) 173.
- [26] C. Anandan, V.K. William Grips, K.S. Rajam, V. Jayaram, P. Bera, *J. Appl. Surf. Sci.* 191 (2002) 254.
- [27] S. Survilienė, V. Jasulaitienė, A. Češūnienė, A. Lisowska-Oleksiak, *Solid State Ionics* 179 (2008) 222.
- [28] N. Mattoso, V. Fernández, M. Abbate, *Electrochem. Solid-State Lett.* 4 (4) (2001) C20.
- [29] S.M. Kumar, A.V.R. Singh, N. Adya, *J. Mater. Eng. Perform.* 17 (5) (2008) 695.